ITALIAN NATIONAL RESEARCH COUNCIL
"NELLO CARRARA" INSTITUTE FOR APPLIED PHYSICS
CNR FLORENCE RESEARCH AREA
Italy

TECHNICAL, SCIENTIFIC AND RESEARCH REPORTS

Vol. 1 - n. 64-11 (2009)

Fulvio Ratto, Paolo Matteini,
Francesca Rossi, Roberto Pini

ANALYSIS OF SECOND HARMONIC GENERATION POLARIZATION PROFILES: AN ATTEMPT TO DEVISE A COMPLETE THREE-DIMENSIONAL MODEL

CNR-IFAC-TR-09-2/009

ISSN 2035-5831

Istituto di Fisica Applicata "Nello Carrara" - CNR
Via Madonna del Piano 10
50019 Sesto Fiorentino

ISSN 2035-5831
Commessa: INT.P07.001 Biofotonica ed Optoelettronica per l'innovazione industriale

ANALYSIS OF SECOND HARMONIC GENERATION POLARIZATION PROFILES: AN ATTEMPT TO DEVISE A COMPLETE THREE-DIMENSIONAL MODEL

Fulvio Ratto, Paolo Matteini, Francesca Rossi, Roberto Pini

Istituto di Fisica Applicata Nello Carrara

Abstract

We report the first attempt to build a three dimensional model of the polarization modulated second harmonic generation and emission dynamics from collagen fibrils under realistic conditions. Our analytical model is constructed by integration of previous knowledge on the stimulation of a second harmonic polarization in a non-centrosymmetric cylindrical target, and on the propagation of a resultant second harmonic disturbance. The application of our paradigm to actual biological targets allows one to retrieve their spatial orientation, mutual organization and inner configuration, which holds great potential to develop biological investigations and theragnostic applications.

1. Motivation

The second harmonic generation (SHG) microscopy is emerging as a promising concept to probe the morphology and functionality of proteins and biological tissues at different organizational levels[1,2]. As a minimally invasive approach, it holds significant potential to become a valuable clinical tool. The use of polarization modulated SHG microscopy may give insight into

properties such as the local orientation, order and inner configuration of assemblies of proteins down to a resolution of a few microns. As a prominent example, collagen exhibits a strong second order nonlinear susceptibility, which translates into a strong SHG signal.[3,4,5,6,7] Since a variety of disorders, incl. e.g. cancer,[8,9,10] involve anomalies in parameters of the collagen molecules and fibrils which may become readily accessible by polarization modulated SHG microscopy, the investigation of SHG signals from collagen bundles has been attracting increasing attention over recent years. Different studies have been devoted to the parameterization of various types of collagen molecules in different kinds of connective tissues. However the interpretation of the polarization modulated SHG signals has been limited to a two dimensional model where all the collagen molecules lie orthogonal to the propagation direction of the laser light (i.e. typically flat on the image plane).[3] In a few connective tissues featuring a high degree of fibrillar alignment, such as e.g. tendons,[11] and under proper experimental setups, this model may represent an excellent approximation of the SHG dynamics. In other connective tissues, the analysis of the SHG signals has been attempted by preliminary manipulations such as e.g. a tentative filtration of the experimental data to reject any misaligned collagen molecule.[8] As a matter of evidence, the lack of a three dimensional model for the SHG signals from collagen molecules and bundles hampers the medical exploitation of this technique, especially in cases where the orientational disorder of the collagen fibrils becomes the parameter of principal clinical relevance.

Here we describe our attempt to devise a three dimensional analytical model of polarization modulated SHG signals from collagen molecules with arbitrary orientation with respect to the propagation direction of the laser light (i.e. under typical conditions, with arbitrary tilt out of the image plane). We prove the advance of our three dimensional analytical model by its application to polarization modulated SHG micrographs of a cross section of a porcine cornea *ex vivo*,[3,12] where the so called lamellae exhibit different orientations with respect to the propagation direction of the laser light.

2. Model description

Let us consider a collagen bundle, which becomes excited by a beam of laser light at frequency ω, impinging the biological target from an arbitrary direction. This beam of laser light induces a polarization P at frequency 2ω, and thus the generation of a second harmonic disturbance. Then the intensity of this second harmonic disturbance becomes detected in the forward direction. We separate the problem into two elemental processes: the generation of the polarization P at

frequency 2ω, and the calculation of the electromagnetic field intensity in the forward direction as due to this polarization *P* at frequency 2ω.

2.1. Generation of a second harmonic polarization

We choose our coordinate system with reference to the collagen bundle frame, so that the principal axis of the collagen bundle is aligned along the *z* axis. On account of the cylindrical symmetry of the collagen bundle, we may take the light propagation direction to rest in the *xz* plane with no loss of generality. Let θ be the angle between the light propagation direction and the *z* axis, i.e. the collagen bundle axis (see Figure 1).

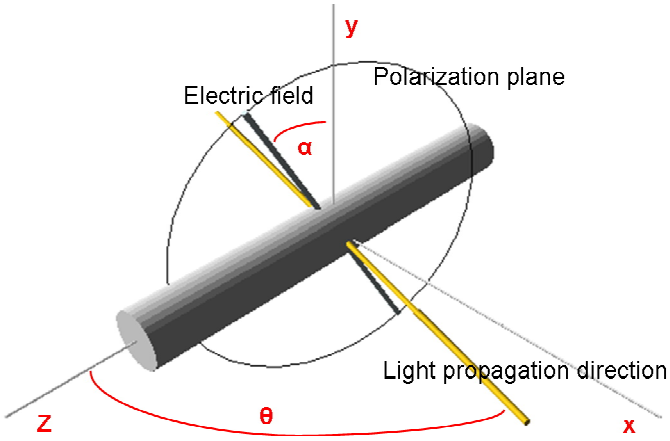

Figure 1: Geometry used in our three dimensional model.

We refer to the discussion in ref. 13 to identify the components of the polarization *P* at frequency 2ω. By virtue of the cylindrical symmetry of the collagen bundle, this can be written as a function of the electric field at frequency ω as:

$$P_x = 2\left(aE_xE_z + bE_yE_z\right)$$
$$P_y = 2\left(aE_yE_z - bE_xE_z\right) \quad ,$$
$$P_z = m\left(E_x^{\,2} + E_y^{\,2}\right) + nE_z^{\,2}$$

Where *a*, *b*, *m* and *n* are the elements of the second order susceptibility tensor of a collagen bundle when aligned along the *z* axis. These elements enclose substantial information on the inner configuration of the collagen molecules, such as the characteristic angles of their triple helix envelope.

Here we whish to parameterize the components of the electric field applied under the experimental conditions realized in the typical polarization profiles. As the linear polarizer is rotated through the scan, the electric field keeps a (quasi) constant intensity, i.e. remains constrained within a (quasi) circular trajectory on a plane perpendicular to the light propagation direction. Therefore this circular trajectory is defined by the angle θ as:

$$\begin{cases} \sin\theta E_x + \cos\theta E_z = 0 \\ {E_x}^2 + {E_y}^2 + {E_z}^2 = E^2 \end{cases}.$$

Under these conditions (θ and E fixed), the electric field becomes completely characterized by another angle α which we refer to the y axis, i.e. the direction within the plane of the circle orthogonal to the collagen bundle.

$$\begin{cases} \theta = \pi/2 & \overline{E} = E(0, \cos\alpha, \sin\alpha) \\ \theta \neq \pi/2 & \overline{E} = E\left(-\sin\alpha / \sqrt{1+\tan^2\theta}, \cos\alpha, \tan\theta \sin\alpha / \sqrt{1+\tan^2\theta} \right) \end{cases}.$$

The angle α (N.B. here referred to the collagen bundle frame) is the parameter which becomes scanned in the typical polarization profiles.

All these equations depict the onset of a polarization P at frequency 2ω as a function of two principal angles: θ is the angle between the light propagation direction and the collagen bundle axis, which belongs both to the collagen bundle frame and to the lab frame; and α is the angle of the electric field relative to the direction orthogonal to the collagen bundle axis, i.e. $\alpha \equiv \alpha^P - \alpha^{c\perp}$, where α^P becomes scanned through the polarization profile and $\alpha^{c\perp}$ belongs to the collagen bundle orientation.

2.2. Emergence of a second harmonic light intensity

Now we use the general formalism introduced in ref. 14 in order to describe the electric field produced by the polarization P at frequency 2ω in the forward direction, at a distance r from the collagen bundle.

We consider two competitive models, based on different possible assumptions on the coherence in the second harmonic generation and emission dynamics. In particular we treat two limit conditions, i.e. a completely coherent and a completely incoherent pictures, according to the principal nature of the collective oscillations at frequency 2ω within the biological target excited by the laser.

2.2.1. Model 1 – completely coherent picture.

The far electric field as due to the polarization *P* at frequency 2ω is described by two orthogonal components over the plane orthogonal to the forward direction, as $\overline{E}_{a,b,m,n}\left(\alpha^{P},\theta,\alpha^{c\perp}\right)=\frac{\mathrm{A}}{r}\left(P_x\cos\theta-P_z\sin\theta,P_y\right)$, where A is a suitable proportionality factor.

We acknowledge the possibility of a partial misalignment and disorganization of the individual collagen molecules within the focal volume excited by the laser, which we describe through an isotropic normal distribution such as:

$$d\wp_{\langle\theta\rangle,\langle\alpha^{c\perp}\rangle,\sigma}\left(\theta,\alpha^{c\perp}\right)=d\theta d\alpha^{c\perp}\Big/2\pi\sigma^{2}\,e^{-\frac{\left(\theta-\langle\theta\rangle\right)^{2}+\left(\alpha^{c\perp}-\langle\alpha^{c\perp}\rangle\right)^{2}}{2\sigma^{2}}}.$$

The width σ of this distribution is a measure of the misalignment of the collagen molecules over the length scale of the focal volume. Next we sum over all the far electric fields produced by all these collagen molecules coherently, and find:

$$\overline{E}\left(\alpha^{P}\right)\equiv\overline{E}_{a,b,m,n}\left(\alpha^{P},\langle\theta\rangle,\langle\alpha^{c\perp}\rangle,\sigma\right)\equiv\iint d\wp_{\langle\theta\rangle,\langle\alpha^{c\perp}\rangle,\sigma}\left(\theta,\alpha^{c\perp}\right)\cdot\overline{E}_{a,b,m,n}\left(\alpha^{P},\theta,\alpha^{c\perp}\right).$$

Finally we calculate the intensity of the second harmonic disturbance as:

$$I\left(\alpha^{P}\right)=\mathrm{B}\left|\overline{E}\left(\alpha^{P}\right)\right|^{2},$$

Where B is another proportionality factor.

Model 1 describes a configuration where all the collagen molecules within the focal volume are completely coherent dipole antennas.

2.2.2. Model 2 – completely incoherent picture.

The far electric field as due to the polarization *P* at frequency 2ω is first decomposed into two incoherent terms, which are associated to the oscillations of *P* along the axis of the collagen bundle and within the plane orthogonal to the axis of the collagen bundle separately: $\overline{E}^{\parallel}{}_{a,b,m,n}\left(\alpha^{P},\theta,\alpha^{c\perp}\right)=\frac{\mathrm{A}}{r}\left(-P_z\sin\theta,0\right)$, $\overline{E}^{\perp}{}_{a,b,m,n}\left(\alpha^{P},\theta,\alpha^{c\perp}\right)=\frac{\mathrm{A}}{r}\left(P_x\cos\theta,P_y\right)$, where A is a proportionality factor.

Then the intensity of the second harmonic disturbance detected in the forward direction is depicted as the summation of the intensities of these two incoherent terms as:

$$I_{a,b,m,n}\left(\alpha^{P},\theta,\alpha^{c\perp}\right)=\mathrm{B}\left(\left|\overline{E}^{\parallel}{}_{a,b,m,n}\left(\alpha^{P},\theta,\alpha^{c\perp}\right)\right|^{2}+\left|\overline{E}^{\perp}{}_{a,b,m,n}\left(\alpha^{P},\theta,\alpha^{c\perp}\right)\right|^{2}\right),$$

Where B is another proportionality factor.

As above, we consider a local configuration where the individual collagen molecules within the focal volume may be partially misaligned, according to an isotropic normal distribution such as:

$$d\wp_{\langle\theta\rangle,\langle\alpha^{c\perp}\rangle,\sigma}\left(\theta,\alpha^{c\perp}\right)=d\theta d\alpha^{c\perp}\Big/2\pi\sigma^{2}\,e^{-\frac{\left(\theta-\langle\theta\rangle\right)^{2}+\left(\alpha^{c\perp}-\langle\alpha^{c\perp}\rangle\right)^{2}}{2\sigma^{2}}}.$$

Then we sum over all the second harmonic components produced by all these collagen molecules incoherently, and find:

$$I\left(\alpha^{P}\right)\equiv I_{a,b,m,n}\left(\alpha^{P},\langle\theta\rangle,\langle\alpha^{c\perp}\rangle,\sigma\right)\equiv\iint d\wp_{\langle\theta\rangle,\langle\alpha^{c\perp}\rangle,\sigma}\left(\theta,\alpha^{c\perp}\right)\cdot I_{a,b,m,n}\left(\alpha^{P},\theta,\alpha^{c\perp}\right).$$

Model 2 describes a configuration where each collagen molecule behaves incoherently with respect to each other. Moreover each collagen molecule is treated as two incoherent dipole antennas, one along the axis of the collagen bundle and one within the plane orthogonal to the axis of the collagen bundle. All these dipole antennas oscillate incoherently, e.g. due to a defect distribution along the collagen filaments as well as inhomogeneities and anisotropies in the dielectric properties of the biological environment.

2.2.3. Comparison of Model 1 and model 2.

Figure 2 displays the modification of the polarization profiles simulated through model 1 (top) and model 2 (bottom), with $\alpha^{c\perp}=0$ and different values of the angles θ (from 90° to 0°, at steps of 10° from top to bottom of all panels) and σ (10°, left and 30°, right), as achieved by use of meaningful values for the elements of the second order susceptibility tensor of the collagen molecules, i.e. $a/n=0.62$, $b/n=0$, $m/n=0.70$.[4] In an attempt to reproduce typical experimental conditions in the construction of average polarization profiles, the curves in Figure 2 where further convoluted by a rectangular profile which represents an angular resolution in α^{P} of 10°.[3]

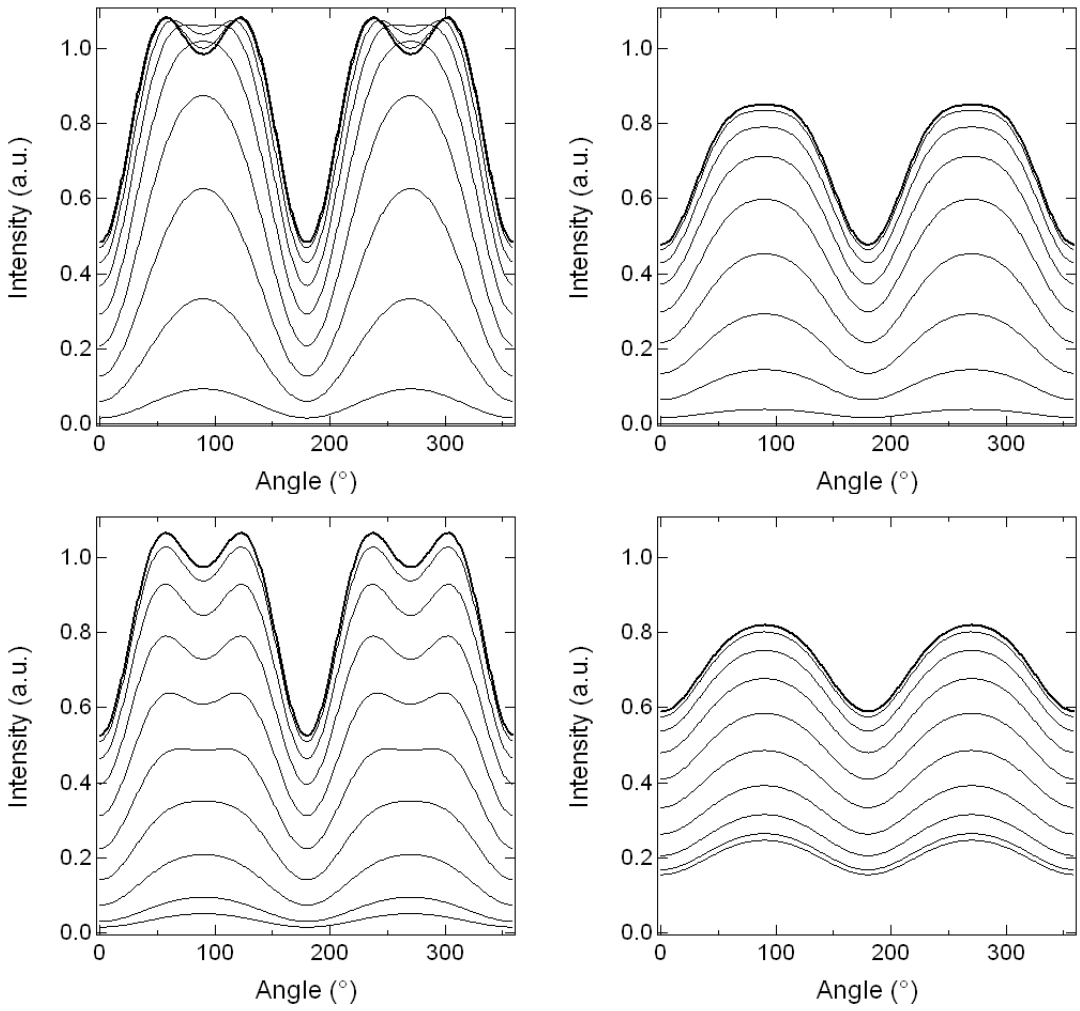

Figure 2: Evolution of the polarization profiles in model 1 (top) and model 2 (bottom) for different values of θ (from 90° to 0° within each panel) and σ (10°, left and 30°, right).

As θ decreases from 90° to 0°, the polarization profiles tend to become less modulated, less structured and less intense. However the qualitative evolution predicted from our two competitive models is different. As θ decreases, the completely coherent picture describes at first a very slow and at last a very fast decrease in the average intensity, with a rapid modification of the structure of the polarization profiles (note the loss of the characteristic horns). Conversely the completely coherent picture depicts a more gradual loss of average intensity and smooth transformation of the structure of the polarization profiles. An increase in σ translates into a loss of modulation and structure of the polarization profiles. Conversely the average intensity decreases at high θ and may increase at low θ. The overall loss of structure and modulation with σ is less pronounced in the coherent picture and more pronounced in the incoherent picture.

3. Comparison with experimental data

Figure 3 shows typical experimental polarization profiles acquired from polarization modulated SHG micrographs of a cross section of a porcine cornea. Since individual polarization profiles acquired from small focal volumes (300 – 400 nm diameter) exhibit poor signal-to-noise ratios, each profile in Fig. 3 is the average over ~ 100 individual profiles with comparable average SHG intensities, i.e. respectively with average SHG intensities within 90 ± 8, 73 ± 8, 55 ± 8, 38 ± 8, and 20 ± 8 % of the maximum found in the frame (upon realignment of each individual profile to set $\alpha^{c\perp} = 0$, within ± 10°). Comparable average SHG intensities are assumed to correspond to comparable values of θ, such that the higher the average intensity the higher the angle θ, as suggested from Fig. 2. The range of intensities displayed embraces most of the range of intensities measured, and so we expect the range of values of θ to represent most of the range from 90° to 0°.

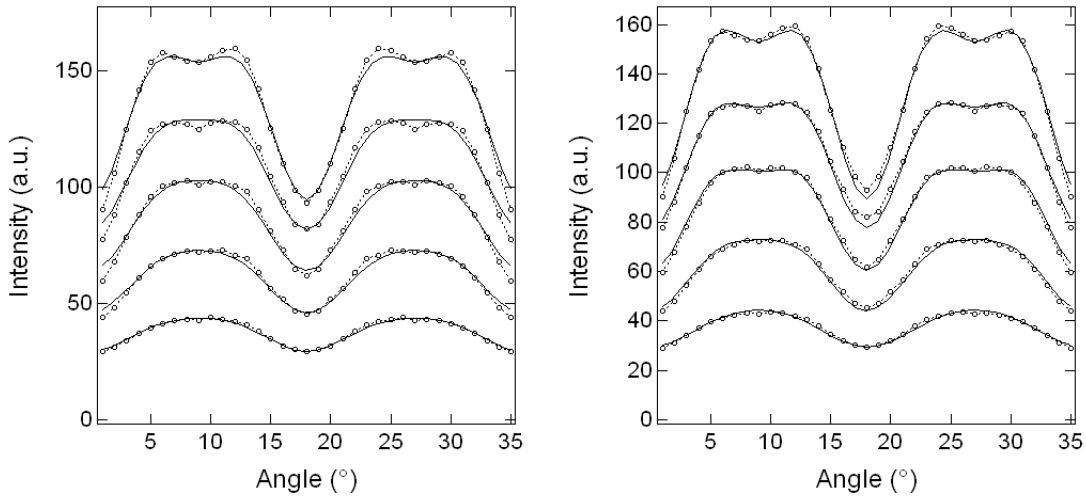

Figure 3: Experimental data fitted with the completely coherent (left) and with the completely incoherent (right) model.

Both our models provide very decent fits of the various experimental profiles, even by use of common values for a/n, b/n, m/n and the proportionality factors (which represent the intensity of the laser light, and so we neglect possible intensity fluctuations) throughout the data series. We notice that model 1 (left) fails to reproduce remarkable fingerprints of the experimental data,

such as the horns about the maxima.[3] Conversely, model 2 (right) provides a fully satisfactory description of the experimental profiles.

Table 1 compares the parameters extracted from our fits with the values expected from the literature and our assumptions.

Parameter	Model 1	Model 2	Expected
a/n	0.74	0.54	(0.62 ± 0.10)[4]
b/n	1.4E-2	-2.2E-6	0[4,13]
m/n	0.87	0.72	(0.70 ± 0.05)[4]
θ (°)	69, 61, 50, 41, 32	85, 66, 53, 40, 20	~ 90… 0
$\langle\sigma\rangle$ (°)	33	17	~ 20[3]

Table 1: Summary of the parameters extracted from our fits.

The expected values for a/n, b/n, m/n were taken from the literature. With regard to θ, we refer to our speculation abut the range of average intensities reported above. The estimate of $\langle\sigma\rangle$ is based on the combination of different factors: ~ 10° is associated with the process of aligning and averaging over the ~ 100 individual polarization profiles, and another ~ 10° results from the actual spread of the orientations of the collagen molecules within the focal volume (300 – 400 nm in diameter), as conjectured from a coherence length of 3 – 4 µm extracted from identical samples.[3]

Overall the picture given by model 2 appears to be more realistic than that by model 1. The reasons why a completely incoherent description of the SHG dynamics proves more accurate is not fully understood at present. (We notice that a semi-coherent model devised as the interplay of mutually incoherent antennas, which yet exhibit internally coherent oscillations over the so-called parallel and orthogonal directions, becomes very comparable to model 1.) We speculate that one such behavior may be associated with high defect densities and strong fluctuations of the dielectric properties of the biological environment, due to its great complexity.

4. Conclusions and perspectives

We have developed a novel analytical paradigm to achieve a complete three dimensional model of the second harmonic generation and emission dynamics from biological targets. We have compared two different assumptions on the coherence of the second harmonic oscillations in collagen fibrils with actual experimental data from the cross section of porcine corneas, and found that an incoherent framework appears to be more appropriate in this case.

Future developments will include the implementation and application of our three dimensional models to different biological targets such as e.g. different collagen fibers, muscle fibers and myofibers, as well as the use of suitable harmonophores with well-controlled orientation and alignment to validate our calculations.

To our knowledge, this is the first attempt to devise and test a three dimensional model of the polarization modulated SHG dynamics from collagen molecules in actual connective tissues. Our results may pave the way to the fruition of the full power of the SHG processes for clinical applications such as the diagnosis of various disorders of connective tissues.

Acknowledgements

We acknowledge G. Toci and M. Vannini for useful discussions and R. Cicchi and F. Pavone for the acquisition of the experimental data

[1] W.R. Zipfel, R.M. Williams, R. Christie, A.Y. Nikitin, B.T. Hyman, W.W. Webb, "Live tissue intrinsic emission microscopy using multiphoton-excited native fluorescence and second harmonic generation," Proc. Natl. Acad. Sci. USA **100**, 7075-7080 (2003).
[2] P.J. Campagnola, L.M. Loew, "Second-harmonic imaging microscopy for visualizing biomolecular arrays in cells, tissues and organisms," Nat. Biotechnol. **21**, 1356-1360 (2003).
[3] P. Matteini, F. Ratto, F. Rossi, R. Cicchi, C. Stringari, D. Kapsokalyvas, F.S. Pavone, R. Pini, "Photothermally-induced disordered patterns of corneal collagen revealed by SHG imaging," Opt. Express **17**, 4868-4878 (2009).
[4] F. Tiaho, G. Recher, D. Rouède, "Estimation of helical angles of myosin and collagen by second harmonic generation imaging microscopy," Opt. Express **15**, 12286-12295 (2007).
[5] R.M. Williams, W.R. Zipfel, W.W. Webb, "Interpreting second-harmonic generation images of collagen I fibrils," Biophys. J. 88, 1377-1386 (2005).
[6] P. Stoller, K.M. Reiser, P.M. Celliers, A.M. Rubenchik, "Polarization-modulated second harmonic generation in collagen," Biophys. J. **82**, 3330-3342 (2002).
[7] S. Roth, I. Freund, "Second harmonic generation in collagen," J. Chem. Phys. **70**, 1637-1643 (1979).
[8] X. Han, R.M. Burke, M.L. Zettel, P. Tang, E.B. Brown, "Second harmonic properties of tumor collagen: determining the structural relationship between reactive stroma and healthy stroma," Opt. Express **4**, 1846-59 (2008).
[9] R. Cicchi, D. Massi, S. Sestini, P. Carli, V. De Giorgi, T. Lotti, and F.S. Pavone, "Multidimensional non-linear laser imaging of basal cell carcinoma," Opt. Express **15**, 10135-10148 (2007).
[10] E. Brown, T. McKee, E. dI Tomaso, A. Pluen, B. Seed, Y. Boucher, R.K. Jain, "Dynamic imaging of collagen and its modulation in tumors in vivo using second-harmonic generation," Nat. Med. **9**, 796-800 (2003).
[11] P. Stoller, B.M. Kim, A.M. Rubenchik, K.M. Reiser, L.B. Da Silva, "Polarization-dependent optical second-harmonic imaging of a rat-tail tendon," J. Biomed. Opt. **7**, 205-214 (2002).
[12] P. Matteini, F. Rossi, L. Menabuoni, and R. Pini, "Microscopic characterization of collagen modifications induced by low-temperature diode-laser welding of corneal tissue," Lasers Surg. Med. **39**, 597-604 (2007).

[13] S.V. Plotnikov, A.C. Millard, P.J. Campagnola, W.A. Mohler, "Characterization of the myosin-based source for second-harmonic generation from muscle sarcomeres," Biophys. J. **90**, 693-703 (2006).
[14] J. Mertz, L. Moreaux, "Second harmonic generation by focused excitation of inhomogeneously distributed scatterers," Opt. Commun. **196**, 325-330 (2001).